ANALYSIS THE INFLUENCING FACTORS OF URBAN TRAFFIC FLOWS BY USING NEW AND EMERGING URBAN BIG DATA AND DEEP LEARNING

Y. Li [1] *, Q. Zhao [2], M. Wang [3]

[1] Urban Big Data Centre, School of Social and Political Sciences, University of Glasgow, Glasgow G12 8RZ, UK - y.li.17@research.gla.ac.uk
[2] Urban Big Data Centre, School of Social and Political Sciences, University of Glasgow, Glasgow G12 8RZ, UK - Qunshan.Zhao@glasgow.ac.uk
[3] School of Geographical and Earth Sciences, University of Glasgow, Glasgow G12 8RZ, UK - Mingshu.Wang@glasgow.ac.uk

KEY WORDS: Traffic Flow, Urban Big Data, Spatial Analysis, Deep Learning, Computer Vision.

ABSTRACT:

Urban traffic analysis has acted an important role in the process of urban development, which can provide insights for urban planning, traffic management and resource allocation. Meanwhile, the advancement of Intelligent Transportation Systems has produced a variety of traffic-related data from sensors and cameras to monitor urban traffic conditions in high spatio-temporal resolution. This research applies spatial regression models combined with computer vision and deep learning to analyse traffic flow distributions via various factors in the urban areas and traffic flow data. We include road characteristics and surrounding environments such as land use/cover, nearby points of interest (POI) and Google Street View images. The results show that the daily average traffic flow on main roads is much higher than smaller roads, and nearby POIs numbers have positive effect on traffic flows. The impact of land cover type is insignificant in the linear regression model, while demonstrates significant contribution to traffic flows in spatial regression models. Although the spatial autocorrelation still exists after the spatial regression, the spatial error model generates a better fit on the dataset. Further analysis will focus on extend the current model with the time parameters and understand what influence the changes of traffic flow in the different spatio-temporal scales.

1. INTRODUCTION

As a crucial component for the complex urban system, urban traffic analysis has drawn attentions from researchers and planners for decades (Batty, 2008). The increasing development of Intelligent Transportation Systems with various urban sensing technologies (Buch et al., 2011), has produced a variety of traffic-related data (Close-circuited television (CCTV) images, cycling counts, and traffic volume data) to monitor urban traffic conditions in high spatio-temporal resolution. These data provide a more real-time understanding of the traffic flows in our cities compared to traditional travel survey methods, which offer the next level of understanding of the urban transportation system.

To analyse the emerging urban big data, computer vision (CV) and deep learning (DL) methods have been used frequently in traffic analysis recently. Some researchers applied DL and CV to measure the city developments by understanding transport modes and pedestrian activities (Ibrahim et al., 2021). A Convolutional Neural Networks (CNN)-based method was proposed to convert traffic information into an image presenting the spatio-temporal features via a two-dimensional matrix (Ma et al., 2017). High accuracy was shown on this image-based traffic speed analysis. The DL coupled with CV has shown advantages over tackling complex issues and processing images more precisely and efficiently. Accurate and timely traffic flow analysis is increasingly significant, as it shows strong demand in individual travellers, business sectors, and government agencies for travel decision, urban planning, and resource allocation.
Many studies measuring the factors that affect urban traffic flows. A research in Yogyakarta, Indonesia was interested in how the speed limit, number of lanes and the density of signalised intersections affected travel time (Irawan et al., 2010). Another study showed the density of bus-stops not only affects the bus speed, but also the speed of other vehicles (He and Zhao, 2013). As a result of having unseparated lanes, non-motor vehicles were shown to have high degree interactions with motor vehicles on the urban road. There is a general consensus that weather conditions significantly affect urban traffic. Researchers introduced a model to predict traffic speed accurately by a comprehensive understanding of rainfall impact (Jia et al., 2017).

Some other urban elements also play an important role in urban mobility analysis. Nian et al. (2010) applied the spatial lag model (SLM) to explore the relationship between Point of Interest (POI) and taxi travels. Xu et al. (2019) proposed a framework to identify urban mobility patterns based on POI data. Another study aggregated the regional POIs by categories to generate an artificial POI-image for each urban grid, which promotes the human mobility prediction at the citywide level (Jiang et al., 2021). In addition to POI, land cover of urban areas also influences the mobility trends. A research using a sequential modelling process to analyse the impact of land use on urban mobility patterns, emissions and air quality (Bandeira et al., 2011). Recently, a study inferred urban land use from taxi trajectory data and bus smart card data (Liu et al., 2021). The variation in the number of origin/destination points over time was initially used to characterize land use types. Besides, street imagery is a new and emerging urban big data source with high spatial resolution. Studies have reported using this data to audit road infrastructure and other built environment features. Goel et al. (2018) used Google Street View(GSV) from 34 cities in Great Britain, to predict travel pattern at the city level.

Previous researchers mostly only explored the multiple aspects of urban environment in qualitative research, like mobility

* Corresponding author

pattern analysis, with limited aspects considered for quantitative analysis, such as factors influence traffic flows. Those existing study overlooks the integrated influence of road characteristics, and other surrounding environments on urban traffic flow, such as land use/cover, nearby points of interest and Google Street View. The analysis of traffic flows plays a crucial role in the process of urban development, providing insights for urban planning, traffic management and resource allocation. To tackle these issues, this research will apply spatial model using DL coupled with CV to analysis the relationship between urban elements (built environment, natural environment, etc.) of the city and traffic dynamic.

2. STUDY AREA AND DATA

2.1 Urban Traffic Flow

The urban traffic flow data are collected from August 5, 2019 to December 05, 2019 by road detectors from Glasgow City Council (GCC). Traffic flow data of GCC area is available from Glasgow Open Data portal (https://gcc.developer.azure-api.net/). During the study period, 1032 sites of traffic flows were recorded, from which 487 valid sites has been used in this research, locating from main road (motorway) to fifth class road (local road), with the time interval of 15 minutes. The detailed data clean process is listed below in the Figure 1. In this research, the traffic data of each site are aggregated as daily average traffic flow across 5 months for further analysis.

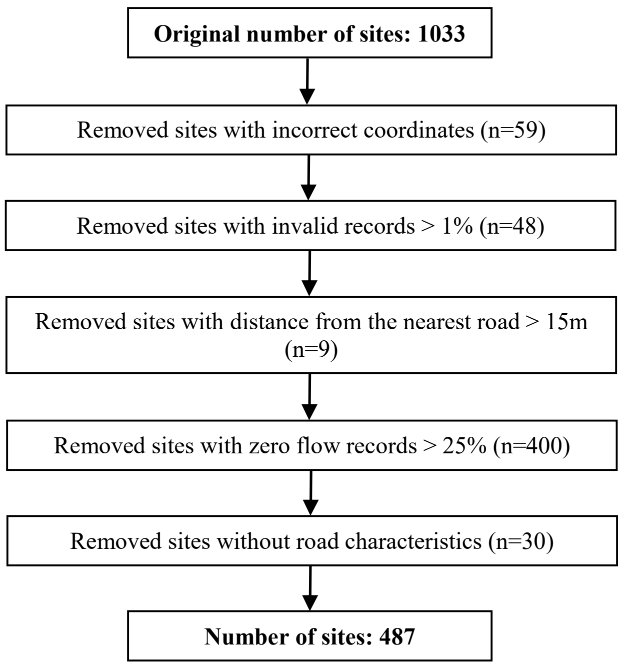

Figure 1. Data cleaning flowchart.

2.2 Urban Road Network and Point of Interest (POI)

Road network data and POI was obtained from Digimap (https://digimap.edina.ac.uk/), a web-based service delivering digital map data and high-quality cartographic products for UK higher education. Road network data provides details of road types, names, directionality, length, width, elevation, start node and end node. POIs of GCC area are categorised into 9 groups, including Retail, Manufacturing and Production, Accommodation, Eating and Drinking, Attractions, Commercial Services, Sport and Entertainment, Transport, Education and Health, and Public Infrastructure. In this research, the number of POIs on each site is calculated within a 100 metres buffer, group with the largest proportion as the major POI of this site.

2.3 Google Street View (GSV)

GSVs of 458 valid traffic flow sites are downloaded from the Street View Static API (https://developers.google.com), provided by Google Maps Platform. GSVs of each site are recorded from 4 perspectives, 0°, 90°, 180°, 270°. This research applies pre-trained DeepLab model from TensorFlow to perform semantic segmentation on GSVs (https://github.com/tensorflow/models/tree/master/research/deeplab). The outputs demonstrate the pixel percentage of 19 typical cityscape objects (Figure 2), from which road, building, vegetation, and car are considered in this research.

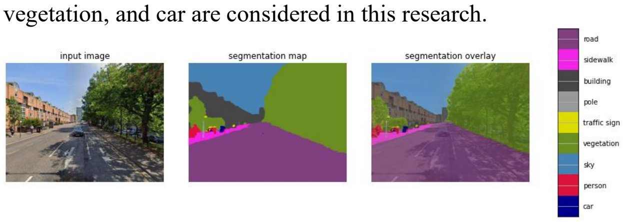

Figure 2. Example output of GSV semantic segmentation.

2.4 Land Cover

The Urban Atlas (https://land.copernicus.eu/local/urban-atlas/) provides comparable land cover and land use data for Functional Urban Areas (FUA) in Glasgow in 2018. The land cover types of GCC area are divided into 27 groups (Figure 3), which are aggregated into 6 categories, including continuous urban fabric, discontinuous urban fabric, green urban areas, industrial, commercial, public, military and private units, roads and railways and others. The image classification is at 10 metres resolution.

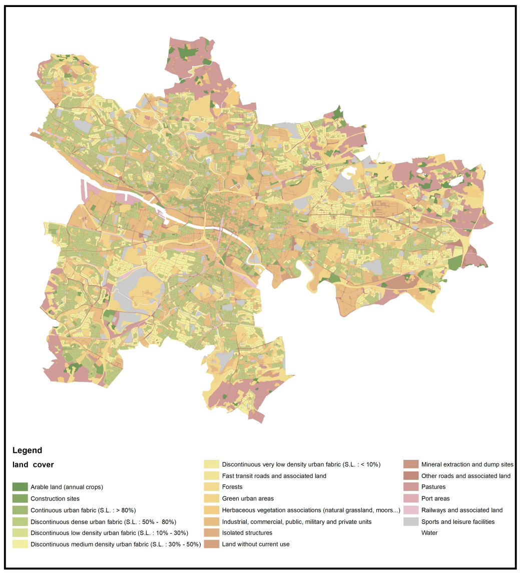

Figure 3. Land cover types of Glasgow.

3. METHODOLOGY

3.1 Semantic Segmentation

Semantic segmentation is a problem of assigning one label l_i to each pixel p_i of an image I, where l_i is one of K different classes.

3.1.1 Object Region Representations: The representations of all the pixels are aggregated weighted by their degrees belonging to the *k*th object region, forming the *k*th object region representation (Yuan et al., 2021):

$$\boldsymbol{f}_k = \sum_{i \epsilon x} \widetilde{m}_{ki} \boldsymbol{X}_i \quad (1)$$

Where $\boldsymbol{X}_i$ is the representation of pixel p_i. $\widetilde{m}_{ki}$ is the normalized degree for pixel p_i belonging to the *k*th object region.

3.1.2 Object Contextual Representations: The relation between each pixel and each object region as below:

$$w_{ik} = \frac{e^{k(X_i, f_k)}}{\sum_{j=1}^{K} e^{k(X_i, f_j)}} \quad (2)$$

Where $k(\mathbf{X}, \mathbf{f}) = \varphi(\mathbf{X})^{\mathrm{T}} \psi(\mathbf{f})$ is the unnormalised relation function, $\varphi(\cdot)$ and $\psi(\cdot)$ are two transformation functions implemented by 1 × 1 conv → BN → ReLU. This is inspired by self-attention for a better relation estimation.

3.1.3 Augmented Representations: The final representation for pixel p_i is updated as the aggregation of two parts, the original representation $\mathbf{X}_i$, and the object contextual representation $\mathbf{Y}_i$:

$$\boldsymbol{z}_i = \mathrm{g}(\boldsymbol{X}_i^{\mathrm{T}}\ \boldsymbol{Y}_i^{\mathrm{T}})^{\mathrm{T}} \quad (3)$$

Where $\mathrm{g}(\cdot)$ is a transform function used to fuse the original representation and the object contextual representation, implemented by 1 × 1 conv → BN → ReLU.

3.2 Regression

3.2.1 Linear Regression Model: A linear regression model will be applied to identify the major elements (built environment, natural environment, etc.) of the urban system influence the spatio-temporal distribution of traffic flows (Seber and Lee, 2012):

$$\boldsymbol{y} = \boldsymbol{X\beta} + \boldsymbol{\epsilon} \quad (4)$$

Where

$$\boldsymbol{y} = \begin{pmatrix} y_1 \\ y_2 \\ \vdots \\ y_n \end{pmatrix} \quad (5)$$

$$\boldsymbol{X} = \begin{pmatrix} x_{11} & x_{12} & \cdots & x_{1m} \\ x_{21} & x_{22} & \dots & x_{2m} \\ \vdots & \vdots & \ddots & \vdots \\ x_{n1} & x_{n2} & \dots & x_{nm} \end{pmatrix} \quad (6)$$

$$\boldsymbol{\beta} = \begin{pmatrix} \beta_1 \\ \beta_2 \\ \vdots \\ \beta_m \end{pmatrix} \quad (7)$$

$$\boldsymbol{\epsilon} = \begin{pmatrix} \varepsilon_1 \\ \varepsilon_2 \\ \vdots \\ \varepsilon_n \end{pmatrix} \quad (8)$$

Where $\boldsymbol{y}$ is a vector of traffic flow on each location; $\boldsymbol{X}$ is a matrix of urban factors (built environment, natural environment, etc.) affecting urban traffic flow in Glasgow; $\boldsymbol{\beta}$ is a vector of regression parameters that to be estimated based on variables and $\boldsymbol{\epsilon}$ represents a vector of unobserved variables, also known as error term for the regression model.

3.2.2 Moran's I Test: Moran's I is a measure of autocorrelation in spatial data and it is used to quantify the autocorrelation in traffic flow residuals of linear regression. The formula can be defined as follow (Draper and Smith, 1998):

$$I = \frac{n}{S} \frac{\epsilon^T \boldsymbol{W} \epsilon}{\epsilon^T \epsilon} \quad (9)$$

Where n is the number of average traffic flows; $\boldsymbol{W}$ is the spatial weight matrix for road links in the network; S is the sum of spatial weights in $\boldsymbol{W}$. if $\boldsymbol{W}$ is row standardised then $\frac{n}{S} = 1$. According to the formula, the value of Moran's I is from 0 to 1, which means the lager the Moran's I is, the more spatial autocorrelation between traffic flow residuals.

3.2.3 Lagrange Multiplier Test: The drawback of Moran's I is that is does not reveal the type of autocorrelation. Currently, there are two types of model are used for analysing the spatial dependence: spatial lag model and spatial error model. Lagrange Multiplier (LM) test is designed to test which type of spatial regression model is most appropriate for the traffic flow data. The LM test can be interpreted as chi-square tests with one degree of freedom. LM test for spatial lag model can be defined as (Darmofal, 2015):

$$LM_{Lag} = \left(\frac{n\boldsymbol{\epsilon}^T \boldsymbol{W} \boldsymbol{y}}{\boldsymbol{\epsilon}^T \boldsymbol{\epsilon}}\right)^2 \left[\frac{n(\boldsymbol{W}\boldsymbol{X}\widehat{\boldsymbol{\beta}})^T M (\boldsymbol{W}\boldsymbol{X}\widehat{\boldsymbol{\beta}})}{\boldsymbol{\epsilon}^T \boldsymbol{\epsilon}} + tr(\boldsymbol{W}^T \boldsymbol{W} + \boldsymbol{W}^2)\right]^{-I} \quad (10)$$

$$M = I - \boldsymbol{X}(\boldsymbol{X}^T \boldsymbol{X})^{-I} \boldsymbol{X}^T \quad (11)$$

LM test for spatial error model takes the form:

$$LM_{Error} = \left(\frac{n\boldsymbol{\epsilon}' \boldsymbol{W} \boldsymbol{y}}{\boldsymbol{\epsilon}' \boldsymbol{\epsilon}}\right)^2 [tr(\boldsymbol{W}' \boldsymbol{W} + \boldsymbol{W}^2)]^{-I} \quad (12)$$

Where n is the number of average traffic flows; $\boldsymbol{\epsilon}$ are the residuals of fitted linear regression model; $\widehat{\boldsymbol{\beta}}$ is estimated parameters of linear regression model; $\boldsymbol{W}$ is the spatial weight matrix for road links in the network; I is the value of Moran's I and tr is the matrix trace operator.

3.2.4 Spatial Error Model: Spatial error model assumes the error terms across different spatial units are correlated, which violates the assumption of uncorrelated error terms in linear regression model. Thus, the spatial error model eliminates the spatial dependence of error terms by including a spatially weighted errors in the error term. The basic form of a spatial error model is (Draper and Smith, 1998):

$$\boldsymbol{y} = \boldsymbol{X\beta} + \boldsymbol{\epsilon} \quad (13)$$

$$\boldsymbol{\epsilon} = \lambda \boldsymbol{W} \boldsymbol{\epsilon} + \boldsymbol{\xi} \quad (14)$$

$$\boldsymbol{\xi} \sim N(0, \sigma^2 \boldsymbol{I}) \quad (15)$$

where $\boldsymbol{W}$ is the spatial weight matrix for detectors, and function of neighbourhood contiguity by distance is applied for identify the neighbours of each detector; $\boldsymbol{\epsilon}$ are the residuals of fitted linear regression model; λ is a scalar autocorrelation parameter and $\boldsymbol{\xi}$ is a vector of mean zero, normally distributed errors. In this case, the weighted sum of errors $\boldsymbol{\epsilon}$ are spatially adjacent to $\boldsymbol{y}$ is included in the error term. Unlike the linear regression model, Maximum Likelihood Estimation (MLE) methods are applied to determine the parameters in the spatial error model.

4. RESULTS

4.1 Distribution of Traffic Flow

4.1.1 Statistical Distribution: A visualisation of the daily average traffic flow in Glasgow from August 5th to December 5th in 2019 has been shown in Figure 4:

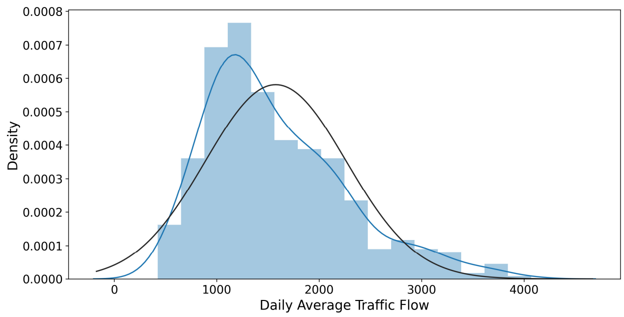

Figure 4. Histogram of daily average traffic flow.

Generally speaking, daily average traffic flow in Glasgow City Council Area follows the normal distribution, which satisfies the null hypothesis of the linear regression model. Besides, it is evident that the median traffic flow along the roads of Glasgow is approximately 1419, while in most areas, there are about 1257 vehicles travelled each day.

4.1.2 Spatial Distribution: It can be observed from the Figure 5 that there is considerable variation in the daily average traffic flow across Glasgow. A spatially West-East divide pattern can be detected that the number of vehicles travelled in the west part of Glasgow generally higher than those travelled in the east part of Glasgow.

The daily traffic flow gets higher towards the centre of Glasgow and lower in peripheral areas, particularly the East and Northeast. However, there is a cluster of high traffic flow visible in the Southeast and the Northeast part of Glasgow, which will be examined using local Moran's I later in detail. Also, there is clear evidence that recorded sites located near to one another tend to have similar traffic flow values, indicating the existence of spatial autocorrelation, which will be examined further in the next section.

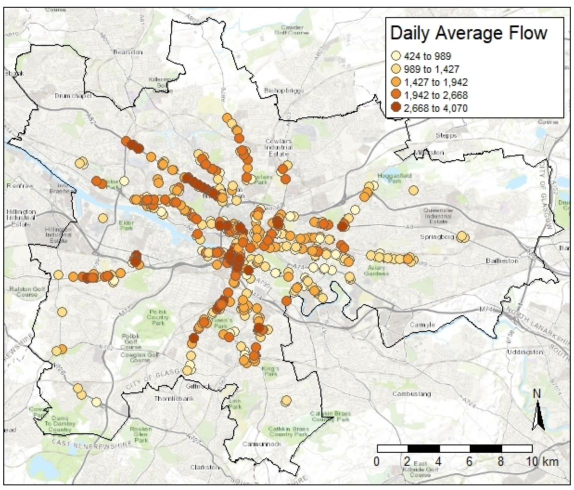

Figure 5. Spatial distribution of daily average traffic flow in Glasgow.

4.2 Linear Regression Model

Before the model implementation, reference categories are selected for each categorical variable, for comparing with other categories. In this study, reference categories are identified as follows:

Variable	Reference Category	Description
Road hierarchy	A road	A major road intended to provide large-scale transport links within or between areas.
POI group	No group	No POI recorded within 100m of the detector.
Land cover	Continuous urban fabric	

Table 1. Reference category

<table>
<tr><th>Variable</th><th>Category</th><th>Estimate</th><th>Std.Error</th><th>Pr(>|t|)</th></tr>
<tr><td>(Intercept)</td><td></td><td>1501.828</td><td>256.953</td><td>9.66e-09***</td></tr>
<tr><td>Road hierarchy</td><td>B road</td><td>-365.147</td><td>112.975</td><td>0.001*</td></tr>
<tr><td></td><td>Local road</td><td>-460.232</td><td>122.991</td><td>0.001***</td></tr>
<tr><td></td><td>Minor road</td><td>-378.286</td><td>76.280</td><td>1.00e-06***</td></tr>
<tr><td>POI number</td><td></td><td>4.436</td><td>1.407</td><td>0.002**</td></tr>
<tr><td>POI group</td><td>Attractions</td><td>963.624</td><td>405.973</td><td>0.018*</td></tr>
<tr><td>Land cover</td><td>Industrial, commercial, public, military and private units</td><td>164.872</td><td>101.456</td><td>0.104</td></tr>
<tr><td>Vegetation (GSV)</td><td></td><td>-3.069</td><td>343.435</td><td>0.992</td></tr>
<tr><td colspan="2">R^2: 0.1417</td><td colspan="3">P-value: 1.688e-05</td></tr>
</table>

Table 2. Linear regression model results (P-value<0.001***)

4.2.1 Results of Linear Regression Model: Table 2 reveals the best model results. The VIF (Variance inflation factor) of different variables are all below 5, it is safe to assume that no multi-collinearity exists within variables. The results of linear regression model of daily average traffic flow demonstrate that some categories of route hierarchy, POI and POI number have significant effect on traffic flows in Glasgow with p-value below 0.05, while land cover type and the coverage of vegetation along the roads have insignificant effect on traffic flow.

As expected, traffic flow on major road (A road) is much higher than other low-level roads. Areas with POI like attractions, which include places of botanical and zoological, historical, and cultural, recreational, tourism and bodies of water, are positive related to the daily traffic flow in Glasgow. Besides, places with high POI number attract more vehicles than lower ones.

This contribution has been peer-reviewed.
https://doi.org/10.5194/isprs-archives-XLIII-B4-2022-537-2022

4.2.2 Residual Analysis of Linear Regression Model: The spatial dependence of linear regression model residuals can be observed from the map below (Figure 6). The residuals of model have similar spatial distribution to daily traffic flow, which demonstrates two significant clusters with low and high values separately.

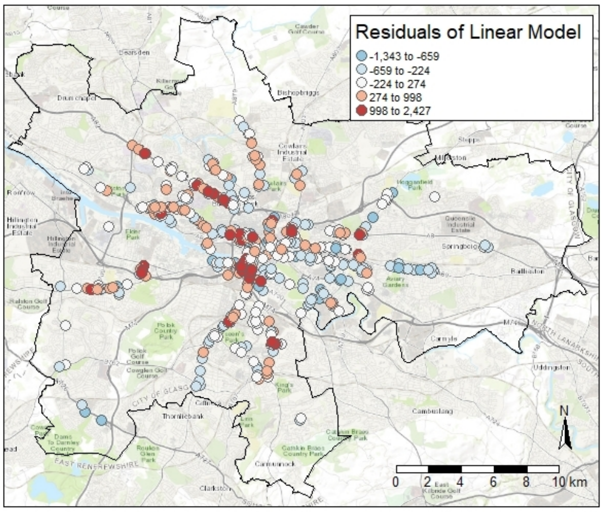

Figure 6. Spatial distribution of residuals of the linear regression model.

The global Moran's I test also justifies that the residuals are spatially auto-correlated ($p < 0.01$). Therefore, the linear regression is insufficient to model the relationship between daily average traffic flow and road factors. A spatial regression model is employed as an alternative

Observed Moran's I	Expectation	Variance
0.0307992444	-0.0021555470	4.0733e-06
P-value: <2.2e-16		

Table 3. Moran's I for regression residuals

4.3 Spatial Regression Model

4.3.1 Lagrange Multiplier Test: The results of Moran's I do not reveal the type of spatial autocorrelation of residuals. Thus, the LM test is applied. The LM test for the spatial lag and the spatial error dependence are designed to test which type of spatial regression model is most appropriate for a given dataset. In this case, the LM test is employed to determine the type of spatial regression model that should be employed to eliminate spatial autocorrelation.

	P-value
Lagrange Multiplier Test for Spatial Lag Dependence	0.2078
Lagrange Multiplier Test for Spatial Error Dependence	0.0016

Table 4. Moran's I for regression residuals

The results of the LM test indicate that the spatial error dependence was significant (p-value < 0.01), while the spatial lag dependence is insignificant with a high p-value. This suggests that the spatial error model is more appropriate for eliminating spatial autocorrelation in the case of daily average traffic flow.

4.3.2 Results of Spatial Error Model: Similar to the linear regression model, the results of the spatial error model on daily average traffic flow demonstrate that some categories of road hierarchy, POI number and POI of attractions have a significant impact on traffic flow along road links with a p-value lower than 0.05. The coverage of vegetation around roads has an insignificant impact on traffic flow (p-value = 0.528). However, in the spatial error model, it shows that vehicles are attracted by places with land cover type of industrial, commercial, public, military, and private units.

The parameter of the spatial error model, Lambda, is significant with p-value of 8.658e-06. Besides, the AIC value of the spatial error model (7714) is lower than that of the linear regression model (7731.8), which indicates that the spatial error model generates a better fit on the dataset.

Variable	Category	Estimate	Std.Error	Pr(>|t|)
(Intercept)		1487.092	376.651	7.87e-05***
Road hierarchy	B road	-383.472	106.366	0.001**
	Local road	-512.777	116.433	1.06e-05***
	Minor road	-417.307	72.043	6.93e-09***
POI number		4.154	1.327	0.002**
POI group	Attractions	951.351	381.939	0.013*
Land cover	Industrial, commercial, public, military and private units	196.439	95.624	0.039*
Vegetation (GSV)		-206.698	327.737	0.528
Lambda: 0.90225	P-value: 8.658e-06	AIC: 7714	AIC for lm: 7731.8	

Table 5. Spatial error model results (P-value<0.001***)

4.3.3 Residual Analysis of Spatial Error Model: It can be seen from Figure 7 that the spatial dependence of residuals is still significant. On the map, there are clusters of residuals with high value around city centre and northwest part of Glasgow. Meanwhile, results of the Moran's I test for residuals indicate that the spatial autocorrelation of residuals is not eliminated (p-value < 0.001). Therefore, we can assume that the spatial dependence of the regression model is not fully accounted for. Overall, it is insufficient to interpret the relationship between daily average traffic flow and urban factors via the spatial error model. More spatial econometric methods such as spatial Dublin model or spatial Dublin error model can be applied further in this analysis.

Observed Moran's I	Expectation	Variance
1.213188e-02	-2.057613e-03	5.102623e-06
P-value: <1.676e-10		

Table 6. Moran's I for residuals of the spatial error model.

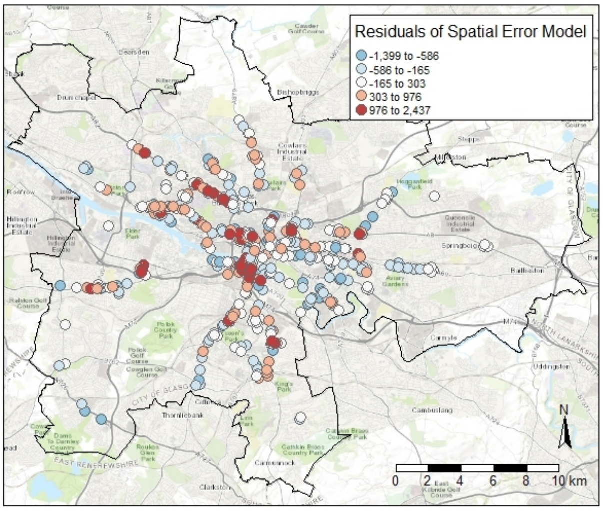

Figure 7. Spatial distribution of residuals of the spatial error model.

5. CONCLUSIONS

The rapid urbanisation in recent years has brought huge impacts on urban traffic due to the growth of urban population, which potentially increases the travel demands and the risk of worsening traffic conditions caused by the overload of the transportation infrastructures. Therefore, urban traffic analysis has acted an important role in the process of urban development, which can provide insights for urban planning, traffic management and resource allocation, and help improve the urban transportation efficiency and living environment.

This research quantifies the urban elements that influence the daily average traffic flow along road links. Deep learning, computer vision and regression models have been applied in this research. The spatial error model used is more appropriate for daily average traffic flow, although with auto-correlated residuals. Both the linear and spatial models suggest that the number of vehicles travelled on main roads are higher than smaller roads. The places with POIs have positive effect on traffic flows, revealing that the more POIs, the higher traffic flows are likely to be. In the contrast, the impact of land cover type with industrial, commercial, public, military and private units is insignificant in linear regression model, while shows significant contributions to traffic flows in spatial error model. Meanwhile, a variation of coverage of vegetation around roads has an insignificant impact on daily average traffic flow in the study area.

ACKNOWLEDGEMENTS

The first author is funded by the China Scholarship Council (CSC) from the Ministry of Education of P.R. China. Dr. Qunshan Zhao has received UK ESRC's on-going support for the Urban Big Data Centre (UBDC) [ES/L011921/1 and ES/S007105/1]. Authors would also like to express their appreciations to the Urban Big Data Centre (UBDC) and Glasgow City Council (GCC) for their data supports.

REFERENCES

Bandeira, J.M., Coelho, M.C., Sá, M.E., Tavares, R., Borrego, C., 2011. Impact of land use on urban mobility patterns, emissions and air quality in a Portuguese medium-sized city. Science of The Total Environment 409, 1154–1163. https://doi.org/10.1016/j.scitotenv.2010.12.008

Batty, M., 2008. The Size, Scale, and Shape of Cities. Science 319, 769–771. https://doi.org/10.1126/science.1151419

Buch, N., Velastin, S.A., Orwell, J., 2011. A Review of Computer Vision Techniques for the Analysis of Urban Traffic. IEEE Transactions on Intelligent Transportation Systems 12, 920–939. https://doi.org/10.1109/TITS.2011.2119372

Darmofal, D., 2015. Spatial Analysis for the Social Sciences. Cambridge University Press.

Draper, N.R., Smith, H., 1998. Applied Regression Analysis. John Wiley & Sons, Incorporated, Newy York, UNITED STATES.

Goel, R., Garcia, L.M.T., Goodman, A., Johnson, R., Aldred, R., Murugesan, M., Brage, S., Bhalla, K., Woodcock, J., 2018. Estimating city-level travel patterns using street imagery: A case study of using Google Street View in Britain. PLOS ONE 13, e0196521. https://doi.org/10.1371/journal.pone.0196521

He, N., Zhao, S., 2013. Discussion on Influencing Factors of Free-flow Travel Time in Road Traffic Impedance Function. Procedia - Social and Behavioral Sciences 96, 90–97. https://doi.org/10.1016/j.sbspro.2013.08.013

Ibrahim, M.R., Haworth, J., Cheng, T., 2021. URBAN-i: From urban scenes to mapping slums, transport modes, and pedestrians in cities using deep learning and computer vision. Environment and Planning B: Urban Analytics and City Science 48, 76–93. https://doi.org/10.1177/2399808319846517

Irawan, M.Z., Sumi, T., Munawar, A., 2010. Implementation of the 1997 Indonesian Highway Capacity Manual (MKJI) Volume Delay Function 8, 11.

Jia, Y., Wu, J., Ben-Akiva, M., Seshadri, R., Du, Y., 2017. Rainfall-integrated traffic speed prediction using deep learning method. IET Intelligent Transport Systems 11, 531–536. https://doi.org/10.1049/iet-its.2016.0257

Jiang, R., Song, X., Fan, Z., Xia, T., Wang, Z., Chen, Q., Cai, Z., Shibasaki, R., 2021. Transfer Urban Human Mobility via POI Embedding over Multiple Cities. ACM/IMS Trans. Data Sci. 2, 4:1-4:26. https://doi.org/10.1145/3416914

Liu, Q., Huan, W., Deng, M., Zheng, X., Yuan, H., 2021. Inferring Urban Land Use from Multi-Source Urban Mobility Data Using Latent Multi-View Subspace Clustering. ISPRS International Journal of Geo-Information 10, 274. https://doi.org/10.3390/ijgi10050274

Ma, X., Dai, Z., He, Z., Ma, J., Wang, Yong, Wang, Yunpeng, 2017. Learning Traffic as Images: A Deep Convolutional Neural Network for Large-Scale Transportation Network Speed Prediction. Sensors (Basel) 17, 818. https://doi.org/10.3390/s17040818

Nian, G., Peng, Bozhezi, Sun, D. (Jian), Ma, W., Peng, Bo, Huang, T., 2020. Impact of COVID-19 on Urban Mobility during Post-Epidemic Period in Megacities: From the Perspectives of Taxi Travel and Social Vitality. Sustainability 12, 7954. https://doi.org/10.3390/su12197954

Xu, Z., Cui, G., Zhong, M., Wang, X., 2019. Anomalous Urban Mobility Pattern Detection Based on GPS Trajectories and POI Data. ISPRS International Journal of Geo-Information 8, 308. https://doi.org/10.3390/ijgi8070308

Yuan, Y., Chen, Xiaokang, Chen, Xilin, Wang, J., 2021. Segmentation Transformer: Object-Contextual Representations for Semantic Segmentation. arXiv:1909.11065 [cs].